[CANCER RESEARCH 64, 4875–4886, July 15, 2004]

Small Molecule Antagonists of the σ-1 Receptor Cause Selective Release of the Death Program in Tumor and Self-Reliant Cells and Inhibit Tumor Growth *in Vitro* and *in Vivo*

Barbara A. Spruce,[1] Lorna A. Campbell,[1] Niall McTavish,[1] Michelle A. Cooper,[2] M. Virginia L. Appleyard,[1] Mary O'Neill,[1] Jacqueline Howie,[1] Jayne Samson,[1] Stephen Watt,[1] Karen Murray,[1] Doris McLean,[1] Nick R. Leslie,[3] Stephen T. Safrany,[3] Michelle J. Ferguson,[1] John A. Peters,[2] Alan R. Prescott,[4] Gary Box,[5] Angela Hayes,[5] Bernard Nutley,[5] Florence Raynaud,[5] C. Peter Downes,[3] Jeremy J. Lambert,[2] Alastair M. Thompson,[1] and Suzanne Eccles[5]

Departments of [1]Surgery and Molecular Oncology and [2]Pharmacology and Neuroscience, The University of Dundee, Ninewells Hospital and Medical School, Dundee; Divisions of [3]Cell Signalling and [4]Cell Biology and Immunology, School of Life Sciences, The University of Dundee, Dundee; and [5]Cancer Research UK Centre for Cancer Therapeutics, Institute of Cancer Research, McElwain Laboratories, Surrey, United Kingdom

ABSTRACT

The acquisition of resistance to apoptosis, the cell's intrinsic suicide program, is essential for cancers to arise and progress and is a major reason behind treatment failures. We show in this article that small molecule antagonists of the σ-1 receptor inhibit tumor cell survival to reveal caspase-dependent apoptosis. σ antagonist-mediated caspase activation and cell death are substantially attenuated by the prototypic σ-1 agonists (+)-SKF10,047 and (+)-pentazocine. Although several normal cell types such as fibroblasts, epithelial cells, and even σ receptor-rich neurons are resistant to the apoptotic effects of σ antagonists, cells that can promote autocrine survival such as lens epithelial and microvascular endothelial cells are as susceptible as tumor cells. Cellular susceptibility appears to correlate with differences in σ receptor coupling rather than levels of expression. In susceptible cells only, σ antagonists evoke a rapid rise in cytosolic calcium that is inhibited by σ-1 agonists. In at least some tumor cells, σ antagonists cause calcium-dependent activation of phospholipase C and concomitant calcium-independent inhibition of phosphatidylinositol 3′-kinase pathway signaling. Systemic administration of σ antagonists significantly inhibits the growth of evolving and established hormone-sensitive and hormone-insensitive mammary carcinoma xenografts, orthotopic prostate tumors, and p53-null lung carcinoma xenografts in immunocompromised mice in the absence of side effects. Release of a σ receptor-mediated brake on apoptosis may offer a new approach to cancer treatment.

INTRODUCTION

The σ receptor has been studied mostly for its functions within the central nervous system, but it is also recognized to be overabundant in many human tumors of neural and nonneural origin (1); this has led to the clinical application of specific small molecule σ ligands in diagnostic tumor imaging (2, 3). Pharmacological studies indicate that there are at least two σ receptor subtypes (4), of which only one (the σ-1 receptor) has been cloned. The σ-1 receptor, at one time viewed as an opioid receptor, has no primary sequence homology to any known receptor class, including classical δ, μ, and κ opioid receptors, from which it is now considered distinct (5). There are, however, close functional connections between σ and opioid receptors (6), in particular, between σ and κ sites (7).

The biology of σ receptors is poorly understood. Small molecules that bind to the σ receptor (σ ligands) are cytotoxic to neural and nonneural cell lines (8), inhibit proliferation in mammary and colon carcinoma and melanoma cell lines (9), and induce apoptosis in colon and mammary adenocarcinoma cell lines (10, 11). There is good evidence that so-called σ-2 agonists induce apoptosis that is caspase independent in mammary carcinoma cell lines (11, 12). This suggests that a putative σ-2 receptor may exert a proapoptotic effect in tumor cells. A nonselective σ ligand that also binds to sterol isomerase, SR 31747, has been reported to have *in vitro* and *in vivo* antitumor activity, but this is not clearly correlated with either σ or sterol isomerase-mediated actions (13).

The importance of programmed cell death (apoptosis) in the prevention and treatment of cancer is well recognized. Most normal cells in the body seem to require a pattern of signals from other cell types to suppress apoptosis (14–16). This is likely to have evolved to maintain correct spatiotemporal patterning during development, but it also serves as a crucial defense against cancer. Cancer cells undergo clonal, unrestrained proliferation, transgress normal tissue boundaries, and migrate to distant parts. To disregard microenvironmental constraints in this way, tumor cells must acquire resistance to apoptosis; otherwise, they would die when deprived of survival support from familiar neighbors (17). It has been proposed that if a tumor's resistance to apoptosis can be overcome, this may expose a vulnerability caused by genetic damage and oncogenic drive, both of which prime tumor cells to undergo programmed cell death. Release of the brake on apoptosis could allow death to be selectively unleashed in tumors but not normal tissues (18).

In this article, we describe the revelation of tumor-selective, caspase-dependent apoptosis by small molecule σ ligands acting through a σ-1 antagonist mechanism. Release of the apoptotic program by inhibitory signaling at the σ-1 receptor is confirmed by σ-1 agonist-mediated rescue of caspase activation and cell death. Normal microvascular endothelial and lens epithelial cells at low passage are as susceptible as tumor cells to σ-1 antagonists, but other normal cells are substantially resistant, including cells such as cerebellar granule neurons that are rich in σ-1 receptors. A unifying feature of susceptible cells is that they share a greater degree of self-reliance compared with most normal cells. We show that cell-selective death appears to be determined by differences in σ receptor coupling in susceptible cells compared with nonsusceptible cells. Death occurs at least partly through σ-1 antagonist-mediated derepression of a proapoptotic pathway that appears to be confined to susceptible cells and is signaled by calcium and subsequent activation of phospholipase C (PLC). In at least some cells σ antagonists also cause calcium-independent inhi-

Received 10/9/03; revised 4/14/04; accepted 5/10/04.

Grant support: Wellcome Trust Clinical Senior Fellowship Grant 033790 (B. Spruce), Wellcome Trust Development Fund Award Grant 058914, Scottish Enterprise Proof of Concept Award Grant 803310, Cancer Research United Kingdom Project Grant C1518/A2678, Breast Cancer Research Scotland Grant 2000/167, and Medical Research Council Cooperative Grant MRC441.

The costs of publication of this article were defrayed in part by the payment of page charges. This article must therefore be hereby marked *advertisement* in accordance with 18 U.S.C. Section 1734 solely to indicate this fact.

Note: S. Safrany is a Royal Society University Research Fellow.

Requests for reprints: Barbara A. Spruce, Department of Surgery and Molecular Oncology, Ninewells Hospital and Medical School, University of Dundee, Dundee DD1 9SY, United Kingdom. Phone: 44-1382-496427; Fax: 44-1382-496363; E-mail: b.a.spruce@dundee.ac.uk.

bition of phosphatidylinositol 3′-kinase pathway signaling that leads to inhibition of protein kinase B (PKB)/Akt. Systemic administration of σ antagonists to immunocompromised mice significantly inhibits the growth of evolving and established mammary, prostate, and lung carcinoma xenografts in the absence of side effects. σ antagonists have been tested in humans for other indications, which could assist the translation of such drugs into human cancer trials.

MATERIALS AND METHODS

σ Ligands and Other Chemicals. σ ligands were obtained from RBI (division of Sigma-Aldrich, Dorset, United Kingdom), Sigma-Aldrich, or Tocris Cookson Ltd. (Bristol, United Kingdom). Rimcazole was obtained from three different sources: RBI (which discontinued marketing of rimcazole during the study); Sigma-Aldrich; and Tocris Cookson. Rimcazole obtained from RBI and Tocris Cookson was water soluble; this enhanced potency particularly *in vivo*. A form of rimcazole that was insoluble in water [(9-[3-(*cis*-3,5-dimethyl-1-piperazinyl)-propyl]carbazole 2HCl.1H_2O] was obtained from Sigma-Aldrich and used during the period when water-soluble rimcazole could not be obtained. Nonwater-soluble rimcazole was dissolved in methanol for *in vitro* assays and suspended in either ethanol or DMSO (with and without cyclodextrin) for *in vivo* assay (as indicated in Fig. 6 legend). Radiolabeled (+)-Pentazocine (28 Ci/mmol) was supplied by NEN (Boston, MA). zVAD.fmk [benzyloxycarbonyl-valinyl-alanyl-aspartyl-(Ome)-fluoromethylketone] was purchased from Calbiochem (Nottingham, United Kingdom). Fura 2-AM was purchased from TEF Laboratories (Austin, TX).

Cell Culture. Continuous mammalian cell lines were obtained from the American Type Culture Collection (Manassas, VA) or the European Collection of Animal Cell Cultures (Porton Down, Salisbury, United Kingdom). Biowhittaker (Clonetics, Inc., Walkersville, MD) supplied primary human cells. The cell lines and primary cells were maintained in the media and supplements recommended by the supplier and incubated at 37°C in a humidified atmosphere of 5% CO_2 in air. Primary cells were tested within the recommended maximum number of population doublings. Primary bovine lens epithelial cells were isolated as follows. Bovine lenses were removed by posterior dissection of the eye, then positioned anterior layer facedown on Sylgard-coated dishes. The posterior capsule and fiber mass were removed, and epithelial cells were removed from the anterior capsule by trypsin. Cells from several lenses were pooled and cultured for three passages before storing in liquid nitrogen. Cells were revived in serum-containing DMEM for experiments. Cerebellar granule neurons were cultured as described previously (19).

Plasmids. pcDNA3 was purchased from Invitrogen (Groningen, the Netherlands). pcDNA3-σ-1 was obtained by subcloning a reverse transcription-PCR (RT-PCR) product from MCF-7 cells (see below). We have previously described pcDNA3-p53 and pSFFV-NEO/Bax (20).

Cell Viability/Proliferation Assay. The MTS CellTitre 96 AQ_{ueous} One Solution Cell Proliferation Assay (Promega, Madison, WI) was used to determine cell viability in control and drug-treated cell populations. This colorimetric assay is dependent on the conversion of the 3-(4,5-dimethylthiazol-2-yl)-5-(3-carboxymethoxy-phenyl)-2-(4-sulfonyl)-2*H*-tetrazolium (MTS) compound to a colored, soluble formazan product in metabolically active cells. Cells were seeded in 96-well microtiter plates at a density of 1×10^5–2×10^5 cells/ml serum-containing (10% FCS) culture medium and left to adhere for ~18 h. Cells were then exposed to σ ligands at a range of concentrations in 10% FCS-containing medium for the duration of the experiment. Cell viability was measured before drug addition and at intervals postdrug addition up to 72 h. The absorbance at 490 nm was read in a Dynex microtiter plate reader (Thermo Labsystems, Ashford, United Kingdom). Cell viability is represented as the ratio of absorbance at time 'x' (postdrug addition) minus drugged blank readings (medium with drug but without cells) over absorbance at time 0 (before drug addition) minus blank readings (medium without drugs or cells), expressed as a percentage. One-hundred percent reflects viable cell numbers at the start of the experiment; values >100% represent net cell proliferation, and values <100% indicate net cell loss (cytotoxicity and not merely cell detachment because the assay measures viable, nonadherent as well as adherent cells).

Colony Formation Assays. H1299 (lung cancer) cells were seeded into 6-well plates and cultured for 48 h until ~70% confluent. Cells were transfected with neomycin resistance-expressing vector DNA using the Lipofectamine method, after which Geneticin (1.5 mg/ml) plus rimcazole (25 μM) or drug vehicle were introduced. After 15 days, colonies were stained with Giemsa and counted.

Caspase Activation Assays. Caspase activation was assayed using the Apo-One Homogeneous Caspase3/7 assay (Promega). Cells were incubated with drug for the time taken to commence engagement of the apoptotic program but before cell loss had occurred. Cells were then mixed with the Homogeneous Caspase 3/7 reagent [prepared by mixing the lysis/permeabilization buffer with the profluorescent caspase substrate—rhodamine 110, bis-(*N*-CBZ-L-aspartyl-L-glutamyl-L-valyl-L-aspartic acid amide—Z-DEVD-R110] and incubated at room temperature for between 1 and 24 h (depending on cell density). The release of fluorescence was measured in a Varian Cary Eclipse Fluorimeter at an excitation wavelength of 485 nm and an emission wavelength of 530 nm. Values were expressed relative to basal levels of apoptosis in untreated cell populations.

RT-PCR. Total RNA was isolated from cell lines and tumor tissue with a Micro RNA Isolation kit (Stratagene, Amsterdam, the Netherlands). Synthesis of first-strand cDNA, and its subsequent amplification was carried out with a Titan One Tube RT-PCR kit (Roche, Mannheim, Germany) using primers (5′-GGATCCCACCATGCAGTGGGCCGTGG-3′ and 5′-GAATTCTCAAGGGTCCTGGCCAAAGAGG-3′), which were designed to amplify the σ-1 receptor open reading frame along with unique *Bam*HI and *Eco*RI sites at the 5′ and 3′ ends of the product. PCR products were subcloned into plasmid vector pcDNA3 for sequencing and expression analysis. To compare the cDNA sequences with those in the GenBank database, BLAST searches were carried out with Entrez (National Center for Biotechnology Information, Bethesda, MD).

Radioligand Binding. Radioligand binding assays on isolated MDA-MB-468 and MCF-7 cell membranes were performed essentially as described previously (1).

Transient Transfection and Quantification of Apoptosis by Flow Cytometric Analysis. These were performed as described previously (20). Parent vector was used to equalize the total amount of DNA in each transfection to control for potential promoter competition effects. The efficiency of transfection was estimated by using one of the reporter plasmids pEGFP-C1 (Clontech, Basingstoke, United Kingdom) or pRSV-βgal.

Calcium Imaging. Single-cell Ca^{2+} imaging was performed using a standard, conventional imaging system (Universal Imaging Corporation) with a Zeiss Axiovert 200 inverted epifluorescence microscope equipped with a ×40 oil immersion objective. Cells were loaded with 3 μM fura-2 AM for 25–30 min at 37°C, in dark conditions in medium containing 120 mM NaCl, 3.5 mM KCl, 0.4 mM KH_2PO_4, 5 mM $NaHCO_3$, 1.2 mM Na_2SO_4, 15 mM glucose, 1.2 mM $MgCl_2$, 1 mM $CaCl_2$, and 20 mM *N*-tris(hydroxymethyl)methyl-2-aminoethane sulfonic acid pH-adjusted to 7.4 with NaOH. Ratiometric images (340/380 nm) were collected at 5–30-s intervals. This was increased to 2-s intervals during the first 5 min of drug application. Numerical data were derived from the somas of 10–20 cells within a field. Data are presented as percentage of change in fluorescent ratio, which is proportional to the intracellular Ca^{2+} concentration.

Visualization of PLCδ1-PH-GFP Localization. MDA-MB-468 cells were grown on coverslips and transfected using Fugene-6 (Roche) with an expression vector encoding a fusion of the pleckstrin homology domain of PLCδ1 with green fluorescent protein (GFP). Cells were maintained in DMEM/10% FCS at 37°C in 5% CO_2 for 24 h before addition of σ ligands. Stimulations were performed under the same conditions, and cells were followed under temperature and humidity-controlled conditions by time lapse fluorescence microscopy (using Improvision Open Lab time lapse software). For static fluorescence micrographs (as depicted in this article), cells were fixed at intervals after addition of drug with 3% w/v paraformaldehyde in PBS. For experiments in buffers +/− calcium, cells were washed twice into prewarmed buffer five min before stimulation. Buffers were as used for calcium imaging. All microscopy used a Leica-inverted stage fluorescence microscope and a Hamamatsu Orca charge-coupled device camera. Images were analyzed using Improvision OpenLab deconvolution software.

Assay of PKB. These experiments followed the protocol described previously (21). During drug incubations all media were adjusted to 1% DMSO. The phosphatidylinositol 3′-kinase inhibitor wortmannin was used at 100 nM as a control for inhibition of cellular PKB activity.

Quantification of Phospholipids. MDA-MB-468 cells were labeled with [^{3}H]myoinositol (50 μCi/ml; Amersham Pharmacia Biotech, Bucks, United Kingdom) in inositol-free DMEM supplemented with 10% dialyzed FCS for 96 h. After treatment with σ ligands or vehicle controls, cells were analyzed for inositol lipid and inositol phosphate content as described previously (22, 23).

Xenografts. Human tumor xenografts were established in immunocompromised host mice as follows: in the first study, MDA-MB-468 mammary carcinoma (estrogen receptor negative) cells were injected s.c. into both flanks of outbred nude (Onu/Onu) mice at 2×10^6 cells (in DMEM)/site. σ ligands (rimcazole, *cis*-U50488 and haloperidol) were administered by daily i.p. injection from day 0 (same day as tumor cell inoculation); control mice received drug vehicle alone. Tumor measurements were made at frequent intervals using Vernier calipers across two perpendicular diameters and tumor volume calculated using the formula ($V = 4/3\ \pi\ [(d1 + d2)/4]^3$) where d1 and d2 are the two diameters. Treatment was continued for 45 days, at which, point the mice were sacrificed, and tumors were excised and weighed. Treated tumor weights were compared with control tumor weights using a two-tailed Mann-Whitney *U* test.

MDA-MB-435 mammary carcinoma (estrogen receptor negative) cells were injected bilaterally into the inguinal fat pads of NCr athymic mice at 1.5×10^6 cells (in DMEM)/site. Treatment with rimcazole was delayed until 7 days after tumor cell inoculation and continued for 24 days. Tumor measurements were made at frequent intervals and tumor volumes calculated as above. Treated tumor volumes were compared with controls in the Mann-Whitney *U* test.

MCF-7 (mammary carcinoma; estrogen receptor positive) or H1299 (lung carcinoma) cells were injected s.c. into the flanks of outbred nude (Onu/Onu) mice at $4–5 \times 10^6$ cells (mixed 1:1 in DMEM with Matrigel Basement Membrane Matrix; Becton Dickinson Biosciences, Oxford, United Kingdom)/site. To promote growth of the tumors derived from MCF-7 cells, the mice were implanted s.c. with 60-day release pellets of 17 β-estradiol (Innovative Research of America, Sarasota, FL), 7 days before the injection of the cells. Rimcazole (by daily i.p. injection) was delayed until tumors had exceeded 40 mm^3 in volume. Tumor volume was calculated from Vernier caliper measurements using the formula given above.

In the orthotopic model of prostate carcinoma, PC3M cells were injected into the ventral prostate of male Ncr athymic mice at 3×10^4 cells/mouse. Rimcazole and IPAG were administered by daily i.p. injection from day 7 after tumor cell inoculation. Treatment was continued for 14 days when primary (prostatic) and secondary (lymph node metastasis) tumors were dissected free of surrounding tissue and weighed. Differences in growth between drug treated compared with control mice were compared using the Mann-Whitney *U* test.

Pharmacokinetic Analysis (Rimcazole). Samples were analyzed by liquid chromatography-mass spectrometry with selected reaction monitoring on a triple quadrupole instrument (TSQ700 Finnigan Incorporation; Hemel Hempstead, Herts, United Kingdom). Plasma and tissue homogenates (in PBS) were extracted by protein precipitation with 3 volumes of methanol, and 25 μl of supernatant were injected into the system. The assay was validated according to the published procedures for analytical validation.

For pharmacokinetic analysis, female Balb/C mice were given a single dose of rimcazole (40 mg/kg body weight) either by oral or i.p. administration. After anesthesia with halothane, blood was taken by cardiac puncture, and liver and splenic tissue samples were taken at intervals postrimcazole administration. For estimation of tumor drug levels (in MDA-MB-435 xenografts), plasma, liver, and tumor drug levels were measured at the end of a 21-day period of daily rimcazole administration (25–26 h after the last drug dose).

RESULTS

Cell-Selective Cytotoxicity of σ Ligands Is Caused by a σ-1 Antagonist Mechanism. We tested a range of tumor cell lines for susceptibility to σ ligands; compounds generally deemed to be antagonists appeared most effective: rimcazole (BW 234U) (24); IPAG (25); reduced haloperidol (26); and BD-1047 and BD-1063 (27). Rimcazole antagonizes the potentiating effects of the σ-1 agonist (+)-SKF-10,047 on neurogenic contractions in the mouse vas deferens, consistent with its classification as a σ-1 antagonist (28, 29). Relative potencies of the σ ligands in proliferation/survival (MTS assays) were, in general, as follows: IPAG>rimcazole>BD-1047 = reduced haloperidol>BD-1063. σ antagonists evoked a concentration- and time-dependent decline in cell viability in tumor cells (Fig. 1, *A* and *B*). In contrast, a range of normal (human) cell types cultured at early passage and seeded at the same density as tumor cells were substantially less susceptible to σ antagonists (rimcazole, Fig. 1*A*; rimcazole and IPAG, Fig. 1*E*). In colony formation assays, rimcazole substantially inhibited the ability of H1299 (p53-null lung carcinoma) cells to form colonies over a period of 2 weeks (Fig. 1*C*).

In an analysis conducted by the National Cancer Institute, rimcazole's IC_{50} (GI_{50}) values (the concentration of drug required to produce a 50% reduction in growth over 48 h) across a panel of tumor cell lines (from the NCI60 panel) ranged from 1.9 to 38 μM (see below). In this study, water-soluble rimcazole was used. We also tested a σ-2 agonist, ibogaine (30), and confirmed that this was cytotoxic to tumor cells as previously reported (11); however, it appeared to be less potent than at least some σ antagonists (ibogaine IC_{50}, 50–100 μM). Prototypic σ-1 agonists, (+)-pentazocine and (+)-SKF-10,047 (31), did not compromise tumor cell viability.

To test whether tumor cell killing was being mediated specifically by antagonism at σ-1 sites, we exposed tumor cells to rimcazole and IPAG in the presence of two prototypic small molecule σ-1 agonists, (+)-SKF10,047 and (+)-pentazocine. The specificity of these ligands for σ-1 sites was confirmed by a recent σ-1-knockout study in mice. In homozygous σ-1-knockout mice, (+)-pentazocine binding to isolated brain membranes is abolished; furthermore, (+)-SKF10,047-mediated stimulation of locomotor activity is not observed in homozygous mutants (32). In our study, both (+)-pentazocine and (+)-SKF10,047 substantially preserved cell viability in tumor cells exposed to σ antagonists (Fig. 1*D*). Agonist-mediated protection was observed even at subequivalent concentrations of agonist relative to antagonist (Fig. 1*D*). In addition, agonist alone sometimes revealed a pronounced proproliferative effect (Fig. 1*D*, *right panel*). In tumor cells, maximal protection from death required incubation of cells with the agonist for ~30 min before addition of antagonist. These findings indicate that the σ-1 receptor, at least in tumor cells, can respond to agonistic signals that drive both proliferation and survival.

Although some normal cell types such as dermal fibroblasts and mammary epithelial cells survived and continued to proliferate in the presence of σ antagonists (Fig. 1*E*, *top panels*), adult dermal microvascular endothelial and bovine lens epithelial cells resembled tumor cells in being susceptible to these agents (Fig. 1*E*, *bottom panels*). Human lens epithelial cells have since been confirmed to be at least as susceptible as bovine lens epithelial cells to σ antagonists (data not shown). In microvascular endothelial cells, as in tumor cells, rimcazole and IPAG-induced death was prevented or at least substantially attenuated by two prototypic σ-1 agonists (+)-pentazocine (Fig. 1*E*, dotted lines, *bottom left panel*) and (+)-SKF10,047 (data not shown). In contrast to tumor cells, rescue was revealed when agonists and antagonists were coadministered, suggesting that the σ-1 receptor is differentially regulated in microvascular compared with tumor cells, subcellular localization differences being one possible reason (33).

σ Antagonists Induce Caspase-Dependent Apoptosis. The time course of death in response to σ antagonists, at least in the lower concentration range, suggested induction of an apoptotic program that is typically engaged many hours or even days after a signal to die. zVAD.fmk, a cell permeable broad spectrum caspase inhibitor, substantially preserved or extended cell viability when measured in MTS assays (Fig. 2*A*). Apoptotic cell numbers were also substantially reduced in the presence of the caspase inhibitor (Fig. 2*B*). Thus, σ antagonists induce apoptosis that is at least partly caspase-dependent apoptosis, unlike σ-2 agonists, which have been reported to induce caspase-independent apoptosis (11).

Activation of caspases in tumor cells in response to rimcazole was

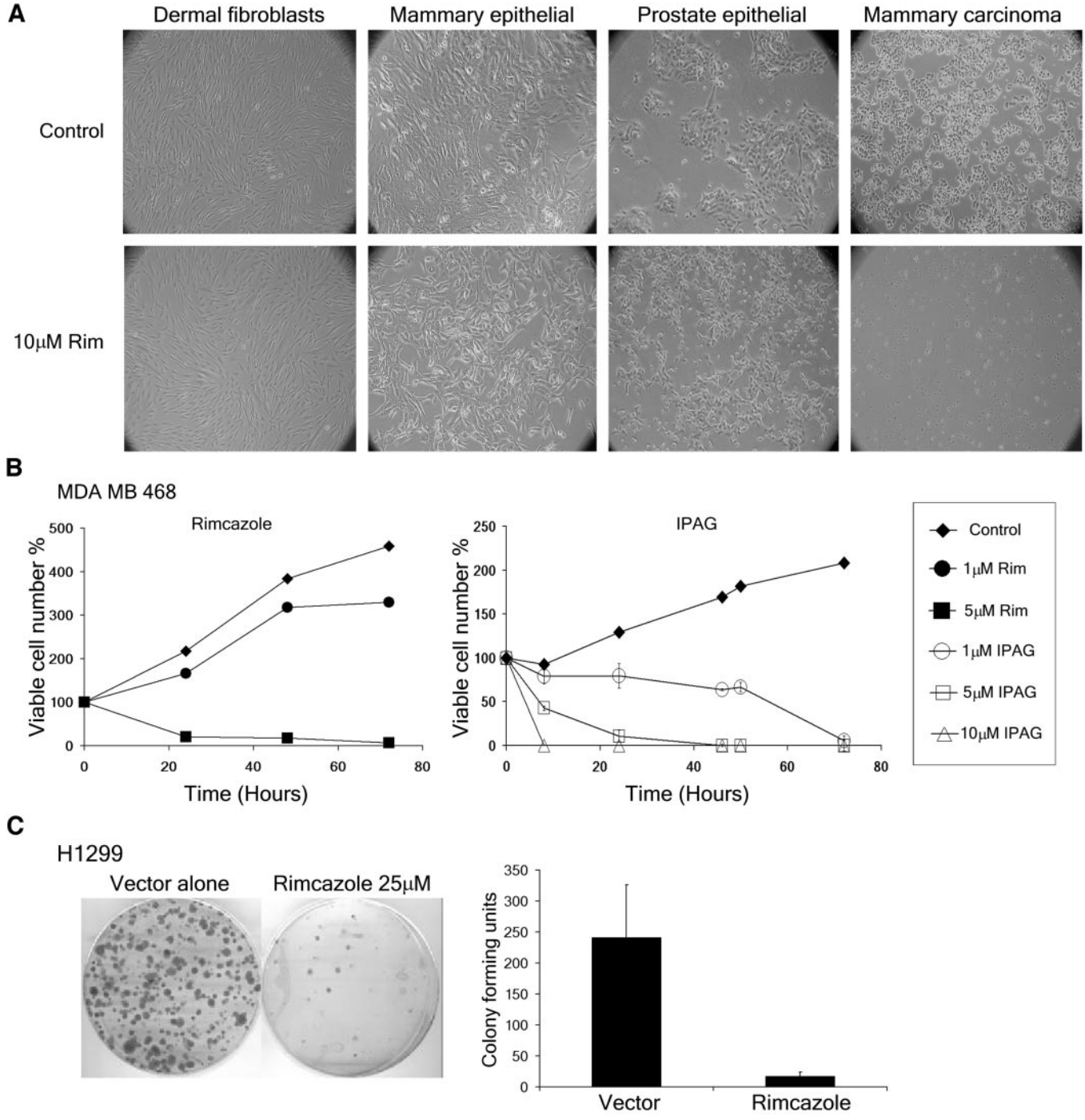

Fig. 1. σ ligands unleash death selectively in tumor, microvascular endothelial, and lens epithelial cells through antagonism at σ-1 sites. *A*, σ antagonists selectively kill tumor cells and spare normal cells. A range of human nontumor cells at low passage were compared alongside human tumor cells, at the same cell density, for susceptibility to σ antagonists. Digital phase contrast micrographs are displayed of human adult dermal fibroblasts, adult mammary epithelial cells, adult prostate epithelial cells, and mammary carcinoma (MDA-MB-468) cells exposed to rimcazole (Rim) for 48 h (*bottom panels*), compared with cells that had received drug vehicle alone (*top panels*). *B*, a representative cytotoxicity assay of a tumor cell line (MDA-MB-468, estrogen receptor-negative mammary carcinoma) grown in high serum (10% FCS) and exposed to a range of concentrations of the σ antagonists Rim (*left panel*) and IPAG (*right panel*) over a 72-h time course. Changes in cell viability were measured by the 3-(4,5-dimethylthiazol-2-yl)-5-(3-carboxymethoxy-phenyl)-2-(4-sulfonyl)-2*H*-tetrazolium (MTS) assay. Each data set was obtained from a representative experiment performed at least three times. Data points represent mean values (±SD) from wells in triplicate or quadruplicate expressed relative to values at time 0 (predrug addition); numbers > 100% reflect net cell number increase, and numbers < 100% indicate a net decline in cell number relative to pretreatment cell numbers over time. *C*, σ antagonists inhibit colony formation *in vitro*. H1299 lung carcinoma cells were transfected with neomycin resistance-expressing plasmid and treated with the neomycin analogue Geneticin in the presence and absence of Rim. After 2 weeks, surviving colonies were stained with Giemsa and viewed by phase contrast microscopy (*left*) and counted as colony-forming units/well (*right*). Values represent mean ± SE from three transfections. *D*, σ antagonist-induced tumor cell death is rescued by two prototypic σ-1 agonists. MCF-7 mammary carcinoma cells were exposed to Rim in the presence (---) and absence (—) of two prototypic σ-1 agonists, (+)-SKF10,047 and (+)-pentazocine. Cells were preincubated with 1 μM agonist for 30 min before addition of antagonist. Changes in cell viability were followed in the MTS assay. Data points represent mean values (±SD) from triplicate or quadruplicate wells in a representative experiment. Deviation bars are not visible because they were smaller than the symbol size. Control cells were exposed to σ antagonist drug vehicle in the presence and absence of agonist. *E*, microvascular endothelial and lens epithelial cells resemble tumor cells in being susceptible to σ-1 antagonists. Human adult male dermal fibroblasts, adult mammary epithelial cells, adult dermal microvascular endothelial cells, and bovine lens epithelial cells at low passage were exposed to 10 μM concentrations of the σ-1 antagonists Rim and IPAG for up to 72 h. Change in cell viability over time was measured in the MTS assay; data points represent mean values (±SD), obtained from wells in triplicate, expressed relative to baseline (pretreatment) values. Graphs depict representative experiments, performed at least three times. Microvascular endothelial cells were protected from Rim and IPAG by coadministration of equimolar concentrations of two prototypic σ-1 agonists (+)-pentazocine (PTZ, ---) and (+)-SKF10,047 (data not shown). Water-soluble Rim was used in experiments depicted in Fig. 1, *A–C*; nonwater-soluble rimcazole was used in Fig. 1*D*.

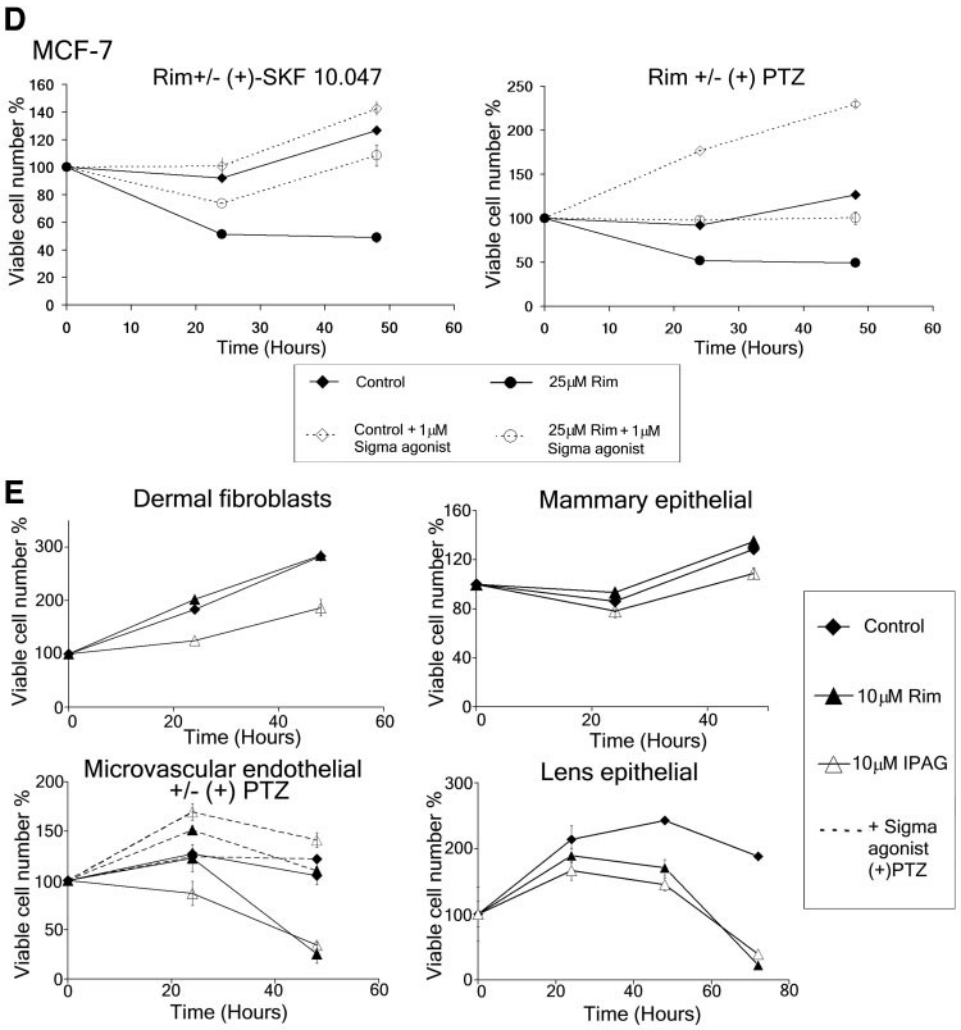

Fig 1. Continued.

confirmed by cleavage of a pro-fluorescent substrate of the tetrapeptide DEVD (Fig. 2*C*; caspase activity expressed relative to untreated control values). Rimcazole-induced caspase activation was prevented by preincubation of cells with subequivalent concentrations of the σ-1 agonists (+)-pentazocine and (+)-SKF10,047 (Fig. 2*C*). This is consistent with a model that death induction is caused by specific antagonism of σ-1 sites that derepresses a signaling pathway culminating in caspase activation. The revelation of DEVDase activity in MCF-7 cells, a caspase-3 null cell line (34) indicates an involvement of the effector caspase-7 that also cleaves DEVD and is thought to be able to substitute at least partly for caspase-3 in its absence (35).

The σ-1 Receptor Is Expressed in Tumor Cells and Confers an Antiapoptotic Drive, but Expression Levels Do Not Correlate with Susceptibility to σ Antagonists. RT-PCR analysis of MDA-MB-468 and MCF-7 mammary carcinoma cells, using σ-1 receptor-specific primers, confirmed expression of the σ-1 receptor in these cells and also in low-passage human primary mammary epithelial cells (Fig. 3*A*). Thus, the mere presence of the σ-1 receptor is not sufficient to determine susceptibility to σ antagonists. Radioligand binding assays confirmed the presence of σ-1 sites (bound by the specific σ-1 ligand, [^{3}H](+)-pentazocine) on both MDA-MB-468- and MCF-7-isolated cell membranes. Rimcazole displaced [^{3}H](+)-pentazocine from MDA-MB-468 membranes with an IC_{50} of 2.7 ± 1.8 μM (mean ± SE), which correlates well with its IC_{50} in cytotoxicity assays of this cell line (Fig. 1*B*). Quantification of σ-1 receptor density was obtained by saturation binding isotherm analysis, which indicated a high density of σ-1 sites on MDA-MB-468 membranes (K_D = 7.7 nM; B_{max} = 3250 fmol mg^{-1} protein). Although many normal tissues appear to express σ receptors at lower levels than tumor cells (the rationale behind exploitation of the σ receptor in cancer diagnosis), some normal cells such as cerebellar granule neurons are rich in σ-1 sites (36) but are resistant to early signaling events unleashed by σ antagonists (see below). Furthermore, total membranes from normal mouse brains have a density of σ-1 sites comparable with that in tumors [B_{max} using radiolabeled (+)-pentazocine in excess of 1000 fmol mg^{-1} protein; Ref. 32]. Thus, it seemed unlikely that differences in the susceptibility of tumor cells would be caused by different levels of wild-type σ-1 receptor expression. This was supported by a lack of correlation between susceptibility to rimcazole and σ-1 RNA levels (estimated by Affymetrix microarray) across the NCI60 cell line panel (Fig. 3*B*).

Although σ-1 receptor expression—at least at the level of wild-type mRNA levels—did not correlate with susceptibility to rimcazole, the data overall supported a model whereby rimcazole inhibits a survival drive mediated through the σ-1 receptor and upon which tumor cells are unduly reliant. Consistent with this, we determined that transient overexpression of the σ-1 receptor (cloned by RT-PCR from MCF-7 cells) into HEK 293 cells (20) reduced the apoptotic response to transfected p53 and Bax (Fig. 3, *C* and *D*). The ability of the σ-1 receptor to protect from apoptosis induction by two recognized tumor suppressor genes would be consistent with its involvement in the tumorigenic process.

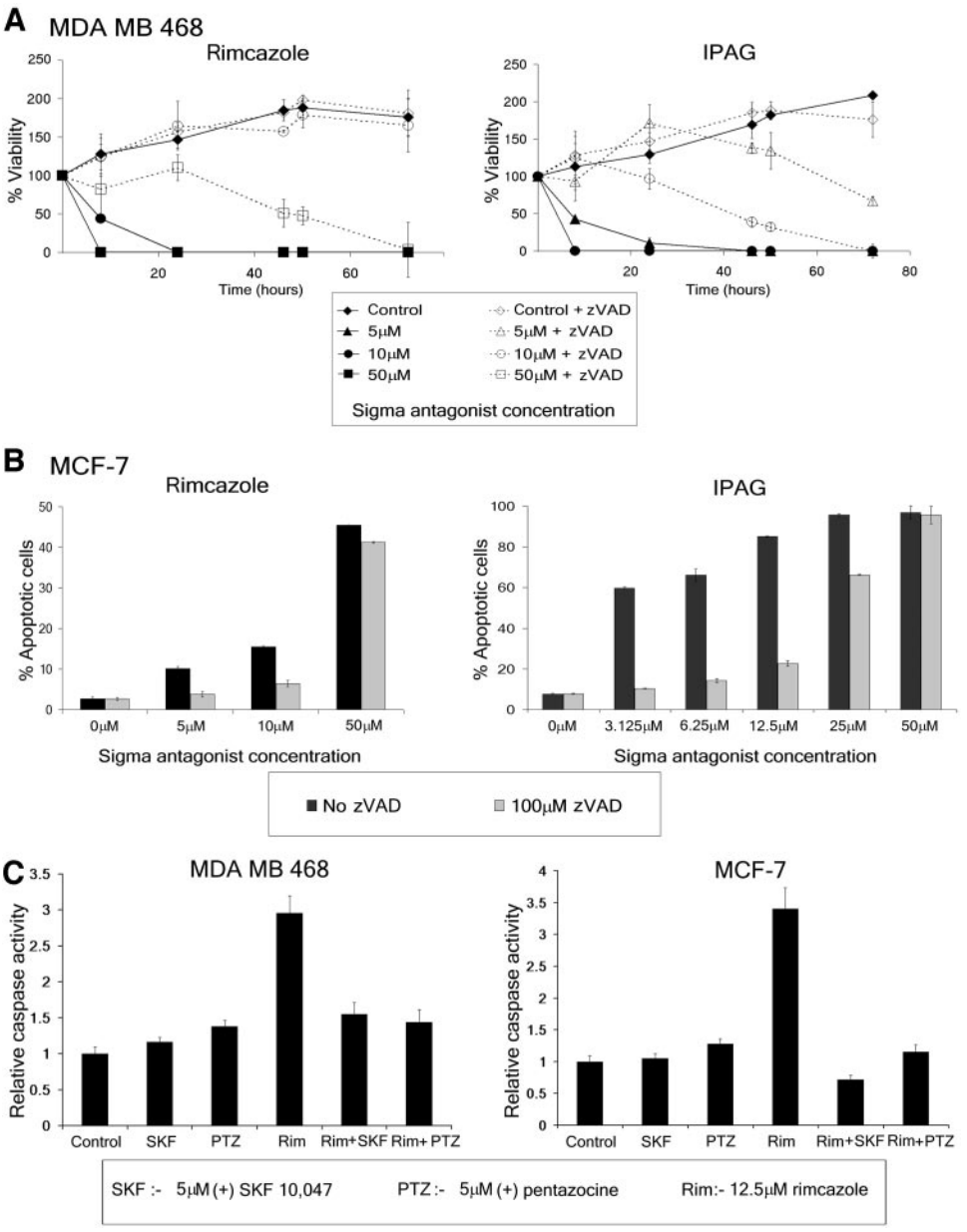

Fig. 2. σ antagonist-induced death is at least partly caspase dependent. *A*, MDA-MB-468 mammary carcinoma cells were exposed to rimcazole (Rim; *left*) and IPAG (*right*) in the presence (*open symbols*) and absence (*closed symbols*) of 100 μM zVAD. fmk, a broad spectrum caspase inhibitor. Changes in cell viability were followed in the MTS assay. Data points represent mean values (±SD) from triplicate or quadruplicate wells. The caspase inhibitor substantially attenuated or delayed death induction by σ antagonists. *B*, MCF-7 mammary carcinoma cells were exposed to Rim (*left panel*) and IPAG (*right panel*) in the presence (▨) and absence (■) of 100 μM zVAD.fmk. After 48 h, cells were fixed, permeabilized, and stained with the nucleic acid dye propidium iodide, then analyzed by flow cytometry to determine the number of cells with subnormal DNA content (sub-G_1 *i.e.*, apoptotic cells) as a percentage of the total cell number. Values represent mean ± SE from samples in triplicate. Numbers of apoptotic cells were substantially reduced in the presence of zVAD.fmk. *C*, Rim induces DEVDase activity that is rescued by σ-1 agonists. MDA-MB-468 (*left*) and MCF-7 (*right*) cells were treated with Rim (12.5 μM), in the presence and absence of σ-1 agonists [(+)-SKF10,047 and (+)-pentazocine (PTZ) at 5 μM, added to cells 30 min before Rim addition] for 18 h. Cell extracts were prepared and incubated with a profluorescent conjugate of DEVD for between 6 and 24 h (at room temperature); activation of caspases 3 or 7 leads to release of fluorescence and caspase activity was calculated as described in "Materials and Methods." Results are expressed relative to basal levels of caspase activity in untreated cell populations (value = 1). Rim-induced caspase activation was prevented by preincubation of cells with σ-1 agonists. Data shown (from a representative experiment) are means ± SDs from wells in triplicate.

σ Antagonists Derepress a Proapoptotic Pathway Signaled by Calcium. Given that the presence of the σ-1 receptor is not sufficient to confer susceptibility to σ antagonists, we reasoned that the response may be determined by the way in which the receptor is coupled in different cell types. The cellular transduction events mediated by σ receptors are unknown. Changes in the concentration of free intracellular calcium ions $[Ca^{2+}]_i$ are recognized to be linked to the induction of apoptosis, but the relationship between $[Ca^{2+}]_i$ and engagement of the apoptotic program is complex because calcium can be a signal for both life and death (37). It has recently been reported that a late supramicromolar elevation in $[Ca^{2+}]_i$ is a common requirement for the execution phase of apoptosis, apparently regardless of the trigger to death (38). However, only a small subset of apoptosis inducers signal through calcium.

Previous studies that the σ-1 receptor associates with the type 3 Ins(1,4,5)P_3 receptor (33) and that σ-2 agonists elevate cytosolic calcium (30) led us to address the potential role of calcium in triggering apoptosis in response to rimcazole and IPAG. In single-cell calcium imaging experiments using the calcium-chelating fluorescent indicator dye fura-2, IPAG evoked a short latency (within seconds) rise in $[Ca^{2+}]_i$ in mammary tumor (MCF-7 and MDA-MB-468) cells (Fig. 4*A*). The rapidity of the $[Ca^{2+}]_i$ response indicated that IPAG was acting as a specific signaler rather than as a nonspecific trigger for the execution phase of apoptosis (38). In contrast to tumor cells, cerebellar granule neurons, cells known to be rich in σ-1 sites (36), consistently displayed little or no increase in $[Ca^{2+}]_i$ after exposure to IPAG (Fig. 4*A*, *right panels*). Thus, the calcium response to σ antagonists is not determined solely by the presence of σ-1 sites.

Single-cell ratiometric calcium imaging enables quantification of the relative increase in $[Ca^{2+}]_i$ after addition of drug. In all cells that died in response to σ antagonists (tumor, microvascular endothelial, and lens epithelial cells), there was a rapid increase in $[Ca^{2+}]_i$ that occurred within seconds and peaked ~2–5 min after drug addition (Fig. 4*B*). Some cancer cells (such as MDA-MB-468 cells) displayed a high basal $[Ca^{2+}]_i$ that underwent spontaneous oscillations (Fig. 4*A*, *top middle panel*); even in these cells there was a marked increase in $[Ca^{2+}]_i$ after drug addition (Fig. 4*B*). In contrast, cells that were

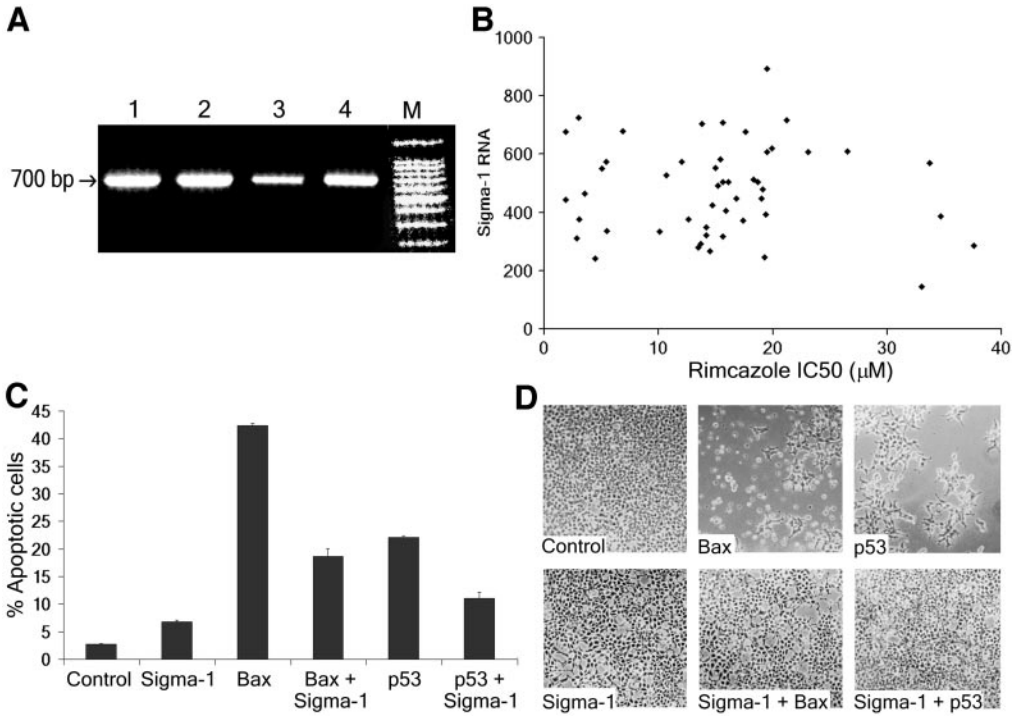

Fig. 3. The σ-1 receptor is overexpressed by tumor cells and confers protection from apoptosis. *A*, reverse transcription-PCR analysis of normal and tumor-derived mammary cells using σ-1 receptor-specific primers designed to anneal to extreme ends of the protein coding region. Seven-hundred bp PCR product isolated from MCF-7 human mammary tumor cells (*Lane 1*), MDA-MB-468 human mammary tumor cells (*Lane 2*), human primary mammary epithelial cells at low passage (*Lane 3*), and Jurkat leukemia cells as positive control (*Lane 4*); loading was standardized from protein concentration of cell lysate; M, size markers. *B*, σ-1 receptor RNA levels do not correlate with susceptibility to rimcazole in the NCI60 cell line panel. IC_{50} (GI_{50}) values for rimcazole were plotted against σ-1 RNA levels (estimated by Affymetrix microarray, NCI identifier GC36876)[6] in individual cell lines. There was an absence of correlation between susceptibility to rimcazole and σ-1 RNA levels (Pearson correlation coefficient, −0.2). *C* and *D*, transient overexpression of the σ-1 receptor protects from apoptosis induction by p53 and Bax. HEK 293 cells were transiently transfected using the calcium phosphate method with vectors encoding the proapoptotic gene products, p53 and Bax, in the presence and absence of vector encoding the human σ-1 receptor. High levels of σ-1 receptor expression were confirmed in radioligand binding assays. Parent vector was used to equalize the total amount of DNA in each transfection and to control for potential promoter competition effects. *C*, 48 h after transfection, cells were harvested and analyzed by fluorescence-activated cell sorting; apoptotic cell numbers were expressed as a percentage of the total cell population. Values were obtained from cells transfected in duplicate or triplicate; each data set was obtained from a representative experiment performed four times. Apoptosis induction after Bax and p53 transfection was substantially attenuated by cotransfection of the σ-1 receptor. *D*, digital phase contrast micrographs of HEK cells 48 h after transfection with vectors encoding p53 and Bax, in the presence and absence of the σ-1 receptor, showing preservation of cells in the presence of the σ-1 receptor.

resistant to σ antagonists such as cerebellar granule neurons and human prostate epithelial cells displayed either no, or a substantially lesser, rise in $[Ca^{2+}]_i$ (Fig. 4*B*).

We went on to confirm that calcium is required for tumor cell death induction by rimcazole and IPAG because viability was retained when cells were exposed to σ antagonists in the presence of 1 μM BAPTA-AM, which crosses the cell membrane to chelate intracellular calcium (Fig. 4*C*). Protection from σ antagonists required preincubation of cells with BAPTA-AM, consistent with the early rise in $[Ca^{2+}]_i$ being required for tumor cell death.

The marked elevation in $[Ca^{2+}]_i$ in tumor cells was selectively revealed by rimcazole and IPAG but not by the σ-1 agonists (+)-pentazocine and (+)-SKF 10,047 and nor by the σ-2 agonist ibogaine (Fig. 4*D*). To confirm that the calcium-raising properties of rimcazole and IPAG are indeed due to specific antagonism of σ-1 sites and not due perhaps to a coexisting σ-2 agonist function of these compounds, calcium responses to σ antagonists were measured in the presence and absence of the σ-1 agonists (+)-SKF10,047 and (+)-pentazocine (Fig. 4*E*). Consistent with cell death assays, coapplication of agonist along with antagonist was insufficient to prevent the rise in $[Ca^{2+}]_i$; however, if cells were incubated with agonist for 30 min before addition of rimcazole or IPAG, there was a substantial attenuation of the $[Ca^{2+}]_i$ rise (Fig. 4*E*). This indicates that the σ-1 agonist is acting to restrain an early calcium rise that signals to apoptosis and is not acting further downstream to rescue death.

σ Antagonists Cause Calcium-Dependent Activation of PLC and a Biochemically Separable Inhibition of PKB/Akt. To address whether the increase in calcium mediated by σ-1 antagonists could have been triggered by a rise in Ins(1,4,5) P_3 from activation of PLC (37), we transfected a fusion protein consisting of GFP coupled to the PH domain of PLCδ1 (PLCδ1-PH-GFP) into MDA-MB-468 cells. The pleckstrin homology domain of PLCδ1 relocalizes from membrane to cytosol when cellular Ins(1,4,5)P_3 concentrations increase and therefore reflects the activity of PLC enzymes in living cells (39). MDA-MB-468 cells containing the PLCδ1- PH-GFP protein were exposed to the σ antagonists IPAG and rimcazole, the σ-1 agonists (+)-pentazocine and (+)-SKF 10,047, and the σ-2 agonist ibogaine. A profound relocalization of the fusion protein from the membrane to the cytosol was induced by exposure to σ antagonists but not agonists (Fig. 5*A*). Using time lapse microscopy, it was apparent that this relocalization occurred within minutes and was maximal within 10 min, after exposure to high concentrations of the antagonists (100 μM). However, at lower concentrations (10 μM) of the ligands it took ~1 h for relocalization to occur, but otherwise, the effect was very similar. In all cases, the relocalization was maintained for at least several hours after addition of the antagonists. Increases in cellular levels of Ins(1,4,5)P_3 and Ins(1,3,4,5)P_4 (240 ± 55 and 277 ± 56, respectively, mean ± SE values as percentages of values in drug vehicle treated cells) and reductions in PtdIns(4,5)P_2 (86 ± 6,

[6] Internet address: http://www.dtp.nci.nih.gov/.

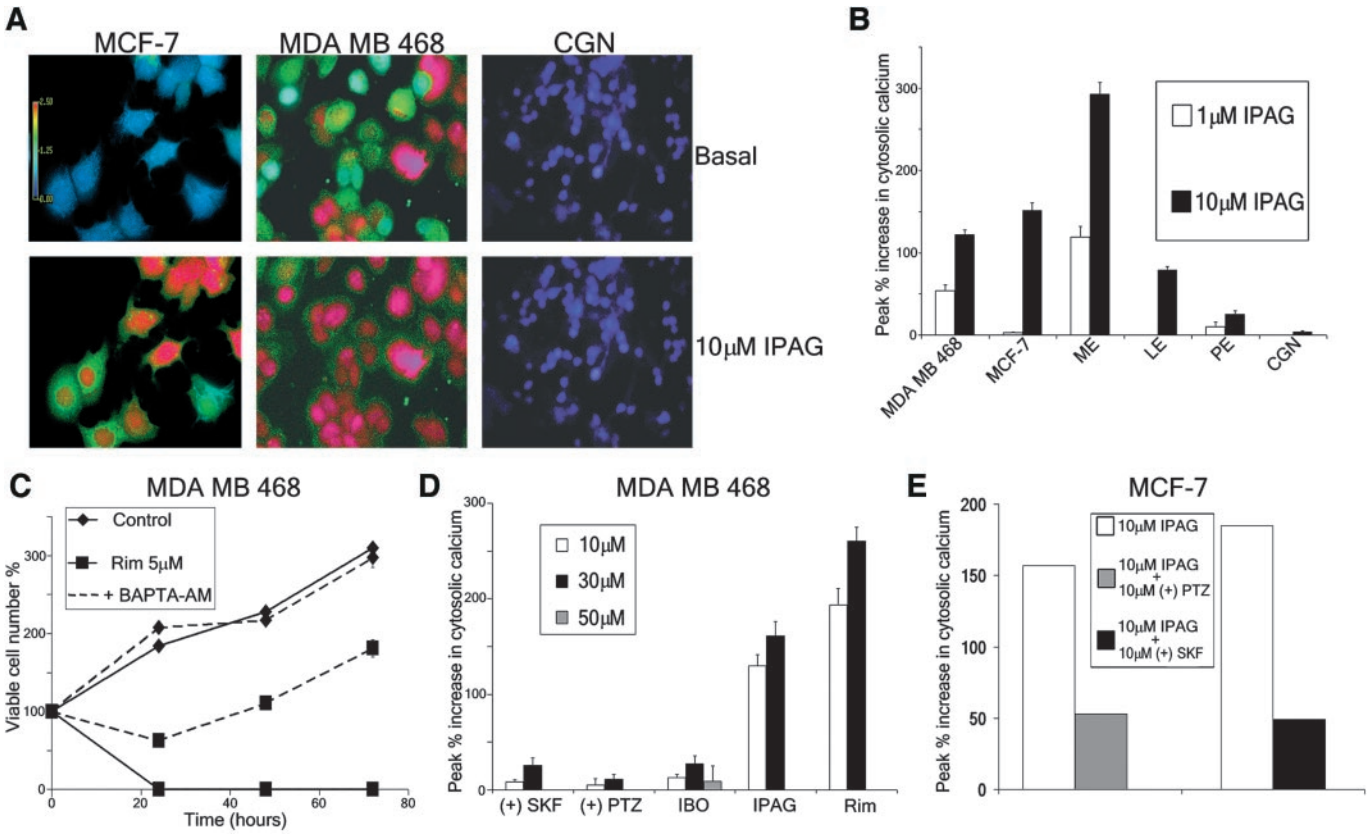

Fig. 4. σ antagonists derepress a cell-selective apoptotic pathway signaled by calcium. *A*, IPAG causes an increase in cytosolic calcium in MCF-7 and MDA-MB-468 cells but not in cerebellar granule neurons. Pseudocolor images are shown that reflect $[Ca^{2+}]_i$ in mammary carcinoma (MCF-7 and MDA-MB-468) cells and cerebellar granule neurons (CGNs) before (*top panels*) and after (*bottom panels*) exposure to 10 μM IPAG at the point of peak elevation in $[Ca^{2+}]_i$. Colors reflect relative $[Ca^{2+}]_i$ as follows: *blue*, low; *green/yellow*, intermediate; *red*, high (see calibration bar). *B*, IPAG concentration dependently elevates cytosolic calcium in mammary carcinoma (MDA-MB-468, MCF-7), primary microvascular endothelial (ME), and primary lens epithelial (LE) cells but not, or to a substantially lesser extent, in other normal cells such as prostate epithelial (PE) cells or CGNs. Data are expressed as the mean peak percentage of change ± SE in the 340/380 nm fluorescent ratio of fura-2. *C*, calcium is required for death induction by σ antagonists. Mammary tumor cells were exposed to rimcazole (Rim) in the presence (---) and absence (—) of 1 μM BAPTA-AM, applied 20 min before the σ antagonist. Change in cell viability over time was followed in the 3-(4,5-dimethylthiazol-2-yl)-5-(3-carboxymethoxy-phenyl)-2-(4-sulfonyl)-2*H*-tetrazolium assay, as above. *D*, σ antagonists but not σ-1 or σ-2 agonists elevate cytosolic calcium significantly in MDA-MB-468 cells. Changes in $[Ca^{2+}]_i$ in MDA-MB-468 cells were estimated after exposure to the σ-1 antagonists IPAG and rimcazole (Rim), the σ-1 agonists (+)-SKF10,047 (SKF) and (+)-pentazocine (PTZ), and the σ-2 agonist ibogaine (IBO). Data are expressed as the mean peak percentage of change ± SE in the 340/380 nm fluorescent ratio of fura-2. *E*, the rise in cytosolic calcium evoked by σ-1 antagonists is attenuated by preincubation of cells with prototypic σ-1 agonists. Peak percentage increase in $[Ca^{2+}]_i$ was measured in MCF-7 cells exposed to 10 μM IPAG alone (□) and after preincubation with (+)-pentazocine (▨) or (+)-SKF10,047 (■) for 30 min before addition of antagonist. Data are expressed as the mean peak percentage of change ± SE in the 340/380 nm fluorescent ratio of fura-2.

mean ± SE percentage of control values) in response to IPAG were demonstrated directly by high-performance liquid chromatography analysis of inositol lipids and soluble inositol phosphates in cells labeled with tritiated inositol; this confirms activation of PLC in response to σ antagonists.

Although activation of PLC can lead to rises in $[Ca^{2+}]_i$, it is also known that large rises in $[Ca^{2+}]_i$ (such as those evoked by capacitative Ca^{2+} entry) can activate the δ isoform of PLC (40). To test whether Ca^{2+} is required for activation of PLC by σ antagonists, the experiments were repeated in nominally calcium-free buffer (which abrogates the rise in $[Ca^{2+}]_i$ in response to σ antagonists in MDA-MB-468 cells; data not shown). Under these conditions, either no or a substantially lesser rise in Ins(1,4,5)P_3 and Ins(1,3,4,5)P_4 was observed (91 ± 20 and 124 ± 20, respectively, mean ± SE values as percentage of control values), and the relocalization of the pleckstrin homology domain fusion protein was also prevented (Fig. 5*B*). Therefore, σ antagonists elevate $[Ca^{2+}]_i$, which in turn leads to activation of PLC, presumptively the δ isoform.

Given that phosphoinositide signaling was modulated by σ antagonists, we investigated the effect of these compounds on the activity of PKB (also known as Akt), a well-characterized phosphatidylinositol 3′-kinase-dependent protein kinase known to promote cellular survival. MDA-MB-468 cells are a particularly suitable system to investigate this because they possess elevated PKB/Akt activity caused by the absence of the tumor suppressor PTEN (41). σ antagonists induced a time- and concentration-dependent decline in immunoprecipitated PKB/Akt activity (Fig. 5*C*). Cellular phosphoinositide measurements showed a significant decline in PtdIns(3,4,5) P_3 levels (56 ± 12, mean ± SE value as a percentage of control value), which would lead to reduced PKB/Akt activity. The decline in PtdIns(3,4,5) P_3 may conceivably be due either to inhibition of phosphatidylinositol 3′-kinase or stimulation of a PtdIns(3,4,5) P_3 phosphatase other than PTEN (because these are PTEN null cells). The reduction in PtdIns(3,4,5) P_3 was not caused by depletion of PtdIns(4,5)P_2 from sustained activation of PLC because neither the inhibition of PKB/Akt (Fig. 5*D*) nor the decline in PtdIns(3,4,5) P_3 was affected by nominal withdrawal of extracellular Ca^{2+}, which does, however, prevent the activation of PLC (Fig. 5*B*). Thus, inhibition of PKB/Akt by σ antagonists appears to be separable from the activation of PLC. It will now be interesting to explore the relative contributions of these two signaling pathways in σ antagonist-mediated death.

Potent and Selective Antitumor Effect of σ Antagonists *in Vivo*. The selective toxicity of σ-1 antagonists for tumor cells *in vitro* prompted us to perform a series of *in vivo* experiments to explore whether σ ligands would influence the growth of human tumor xenografts in immunocompromised mice. We chose rimcazole for

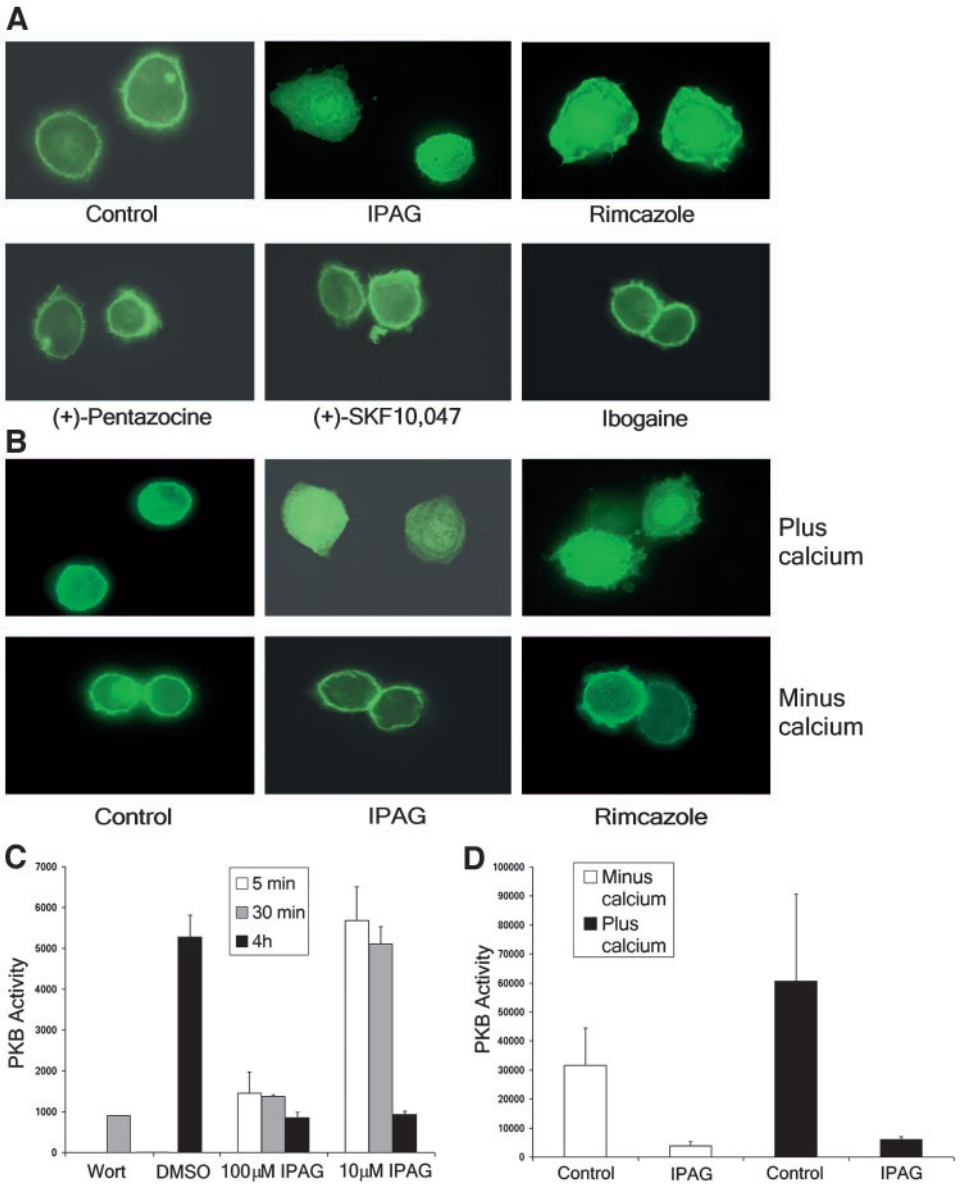

Fig. 5. Sigma antagonists cause calcium-dependent activation of phospholipase C (PLC) and calcium-independent inhibition of protein kinase B (PKB)/Akt. *A*, MDA-MB-468 cells expressing the PLCδ1-PH domain fused to green fluorescent protein were treated with σ antagonists and agonists (as above) for the time taken to cause maximal relocalization (determined previously from time lapse imaging). Cells were then fixed and observed by fluorescence microscopy. *B*, MDA-MB-468 cells expressing the PLCδ1-PH domain fused to green fluorescent protein were incubated with either σ antagonists or drug vehicle alone (DMSO, control) in buffer that contained either 1 mM calcium or was nominally calcium free and then fixed and observed by fluorescence microscopy. *C*, IPAG inhibits cellular PKB/Akt activity. MDA MB 468 cells were treated for the times shown with IPAG, wortmannin (Wort), or DMSO control. Endogenous PKB was then immunoprecipitated and assayed *in vitro*. Data are presented as mean cpm because of labeled phosphate incorporated into the peptide substrate +/− SD from three independent dishes. *D*, inhibition of PKB/Akt is calcium independent. MDA-MB-468 cells were incubated for 30 min in buffer with and without 1 mM calcium and with either IPAG or DMSO control. Endogenous PKB was then immunoprecipitated and assayed *in vitro*. Data shown represent mean cpm +/− SD from four independent dishes.

these initial studies because it was entered into clinical trial for a psychiatric indication some years ago. Therefore, we reasoned that its pharmacokinetics were likely to be favorable, which has been confirmed. After a single dose of rimcazole in mice (40 mg/kg body weight by i.p. or p.o. administration), rimcazole was shown to be absorbed well and was distributed rapidly into tissues, including the liver. Plasma concentrations were comparable after i.p. and p.o. administration (reaching a peak between 2 and 3 μM), and levels within liver peaked in excess of 60 μmol/kg tissue. There was even more pronounced accumulation of rimcazole in tumor tissue (see below).

The efficient clearance of rimcazole from plasma and distribution into tissues indicated good bioavailability following both p.o. and i.p. administration. For practical reasons, we chose the i.p. route for our initial antitumor studies. Systemic (daily i.p.) administration of rimcazole at a relatively low dose of 10 mg/kg body weight significantly slowed the growth of evolving, s.c. hormone-insensitive human mammary carcinoma (MDA-MB-468) xenografts in outbred nude mice (Fig. 6*A*). Despite the potent and sustained inhibition of tumor growth over a period in excess of 6 weeks, during which time rimcazole was administered daily, the mice suffered no overt side effects, thrived, and gained weight. Two additional σ ligands—haloperidol and *cis*-U50488—that we had previously determined to have a cytotoxic effect on MDA-MB-468 cells also slowed xenograft growth. Of these, only *cis*-U50488 produced a degree of tumor slowing that was statistically significant (Fig. 6*A*, *extreme right panel*).

Rimcazole also slowed the growth of pre-established, hormone-insensitive mammary carcinoma xenografts (MDA-MB-435; Fig. 6*B*, *left panel*) in Ncr athymic mice. Rimcazole levels were analyzed in MDA-MB-435 xenograft tumors at the end of the 21-day treatment period and compared with levels in plasma and liver (Fig. 6*B*, *right panel*). Levels were analyzed >24 h after the final drug dose, at which time, plasma concentrations were well below the IC_{50} range (10–70 nM); however, tumor levels remained in the micromolar range and were ~20–100-fold higher than plasma levels (tumor levels ~1100–1600 nmol/kg). Linear pharmacokinetics were suggested by plasma and liver levels after dosing at 30 mg/kg body weight compared with 15 mg/kg body weight (Fig. 6*B*, *right panel*). However, there was a smaller difference in tumor levels, which is consistent with the relative magnitude of the antitumor effect at these dose levels.

Rimcazole also significantly slowed the growth of well-established

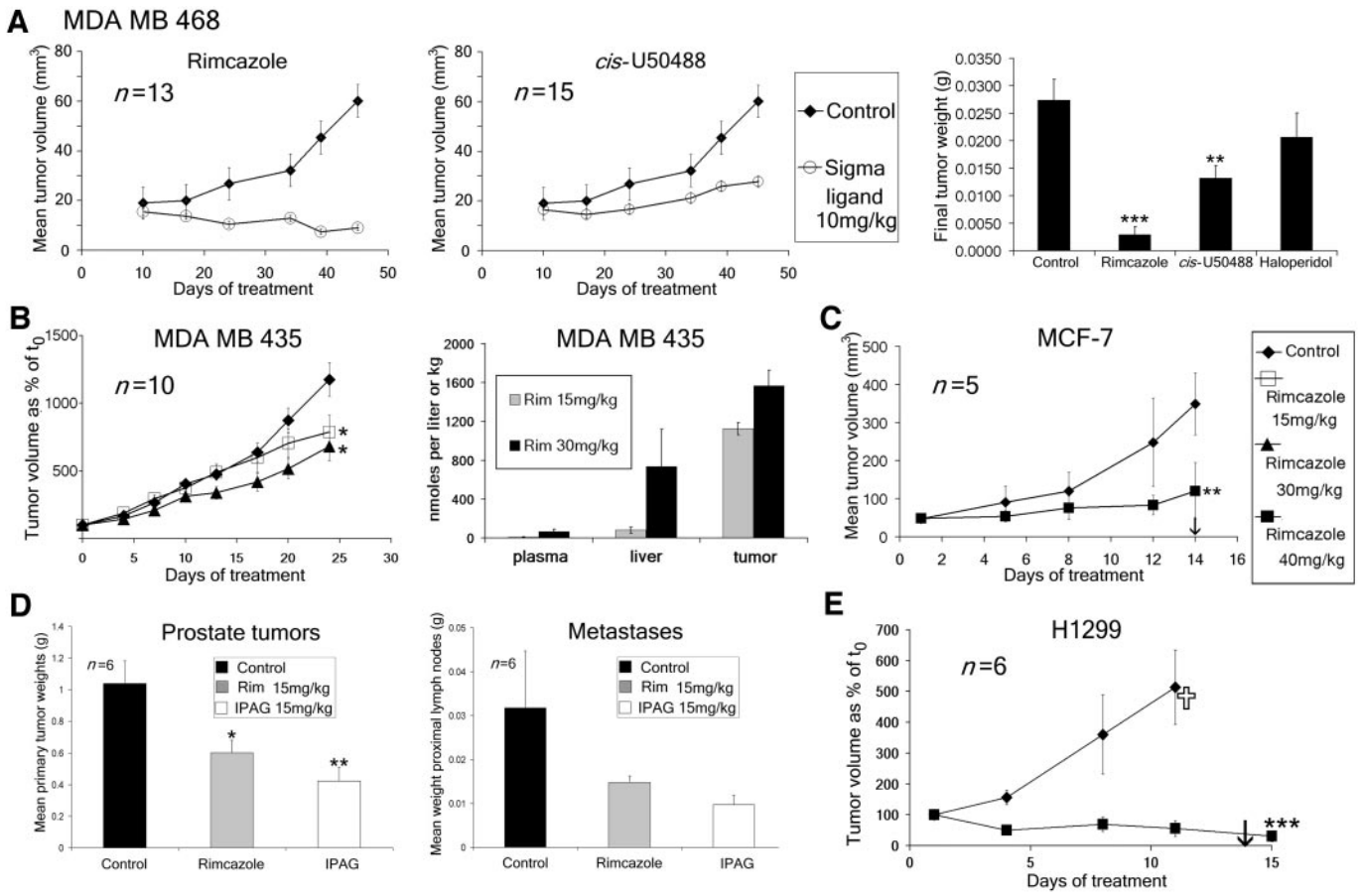

Fig. 6. *In vivo* antitumor effects of σ ligands. *A*, sustained inhibition of evolving hormone insensitive mammary carcinoma xenografts by systemically administered σ ligands. Line graphs depict growth curves of MDA-MB-468 (estrogen receptor negative) human mammary carcinoma xenografts in Onu/Onu (outbred nude) mice. σ ligands—rimcazole (Rim; water soluble), haloperidol, and *cis*-U50488—were administered by daily i.p. injection at a dose of 10 mg/kg body weight. σ ligand treatment was commenced on day 0 (same day as tumor cell inoculation); control mice received drug vehicle alone. Tumor volume measurements are expressed as mean ± SE. The bar graph depicts tumor weights at excision on day 45. Rim- and *cis*-U50488-treated tumors weighed significantly less than control tumor weights ($P < 0.001$ and $P < 0.01$; Mann-Whitney *U* test, two-tailed). *B*, Rim inhibits the growth of established hormone-insensitive mammary carcinoma xenografts and shows accumulation in tumor tissue. MDA-MB-435 (hormone insensitive) mammary carcinoma xenografts were established in Ncr athymic mice. Nonwater-soluble Rim (Aldrich-sourced) was administered by daily i.p. injection at 15 and 30 mg/kg body weight for a period of 21 days. Rim treatment (in DMSO) was delayed until 7 days after tumor cell inoculation; control mice received drug vehicle alone. Tumor volumes were measured at intervals and expressed as a percentage of baseline, pretreatment (t_0) tumor volumes (mean ± SE; *left panel*). Treated tumor volumes differed significantly from controls at both 15 and 30 mg/kg dose levels ($P < 0.05$; Mann-Whitney *U* test). *B, right panel*, Rim levels were measured in plasma, liver, and MDA-MB-435 xenograft tissue at the end of the 21-day treatment period (25–26 h after the last drug dose). Rim levels in tumor tissue were substantially higher than in either liver or plasma at both drug doses. Plasma levels are expressed as nmol/liter (mean ± SE) and liver and tumor levels as nmol/kg (mean ± SE). *C*, MCF-7 (hormone-sensitive mammary carcinoma) xenografts were established in outbred nude (Onu/Onu) mice. Rim (Aldrich-sourced, administered at 40 mg/kg body weight by daily i.p. injection, in ethanol plus cyclodextrin, for 14 days) was delayed until individual tumors had reached a size within the range 40–50 mm^3. Absolute tumor volume (calculated using formula in "Materials and Methods") was measured and compared with values for control tumors that received drug vehicle alone. Treated tumor volumes (mean ± SD) differed significantly from control tumor volumes at the termination of the experiment ($P < 0.01$; Student's *t* test). *D*, Rim and IPAG inhibit the growth of primary and metastatic orthotopic prostate carcinoma xenografts. PC3M prostate carcinoma cells were injected into the ventral prostate of male Ncr athymic mice. Mice were treated with nonwater-soluble Rim and IPAG (both in DMSO) by daily i.p. injection from day 7 after tumor cell inoculation and continued for 14 days when primary (prostatic; *left panel*) and secondary (lymph node metastasis; *right panel*) tumors were dissected and weighed. Both Rim- and IPAG-treated primary tumors were significantly smaller than control tumors at the 15 mg/kg dose level ($P < 0.05$ and $P < 0.01$; Mann-Whitney *U* test, two-tailed). Secondary tumors also appeared to be slowed by Rim and IPAG, but results did not achieve statistical significance. *E*, water-soluble Rim induces regression of well-established p53-null lung carcinoma xenografts. H1299 cells were injected into the flanks of outbred nude (Onu/Onu) mice and allowed to develop into tumors ranging from 40 to 400 mm^3 in volume before commencement of treatment with Rim (Tocris-sourced) by daily i.p. injection; control mice received water (drug vehicle) alone. Tumor volumes were measured at intervals and expressed as a percentage of baseline, pretreatment (t_0) tumor volumes (mean ± SD). Rim-treated tumors were significantly smaller than control tumors at the termination of the experiment ($P < 0.001$; Student's *t* test). Control mice were sacrificed at day 11 due to the large size of their tumors. *Arrow* indicates the day on which Rim treatment was discontinued.

estrogen receptor positive (MCF-7) xenografts in outbred nude mice even over a short period of treatment (Fig. 6*C*). In an orthotopic prostate carcinoma model, systemically administered rimcazole and IPAG slowed the growth of primary tumors and possibly inhibited the growth of metastases in addition (Fig. 6*D*). Using water-soluble rimcazole, well-established, aggressive p53-null lung tumors showed stasis or regression within 2 weeks of commencing treatment (Fig. 6*E*). Differences in the magnitude of the antitumor effect may be due to mouse strain (outbred nude mice displayed better responses in general compared with Ncr athymic), although a contribution from rimcazole formulation differences, and hence solubility, is also possible.

DISCUSSION

Our data support a model whereby inhibition of σ-1 receptor function in tumor, microvascular endothelial, and lens epithelial cells impairs an antiapoptotic drive on which these cells are unduly reliant and is sufficient to release the death program. The mere presence of the σ-1 receptor does not confer susceptibility to σ antagonists because we show that several types of normal microenvironment-constrained cells, including those known to be rich in σ-1 receptors, withstand σ receptor inhibitors. Cells that are resistant to these agents include human low-passage primary mammary epithelial cells, primary prostate epithelial cells, primary dermal fibroblasts, and rodent

cerebellar granule neurons. Primary microvascular endothelial and lens epithelial cells appear, however, to be atypical among nontumor cells in dying in response to σ-1 antagonists. We hypothesize that one element of commonality between susceptible cells is their possession of autocrine signaling pathways that can promote cell survival. Lens epithelial cells differ from most normal cells in being able to survive in the company of like cells alone (42). Dermal microvascular endothelial cells secrete and respond to products of the opioid precursor, proopiomelanocortin, to cause release of interleukin 8 (43), a recognized potent proangiogenic factor (44). Such cells may conceivably need a proapoptotic safeguard to prevent lone cell survival; tumor cells in their efforts to acquire self-reliance may be similarly burdened. The selective susceptibility of tumor, microvascular endothelial, and lens epithelial cells to σ antagonists suggests that even a degree of self-reliance (due perhaps to functional autocrine signaling that is not necessarily the cell's exclusive mode of survival) may confer sensitivity. The susceptibility of microvascular endothelial cells to rimcazole and IPAG is particularly enticing because it suggests that σ antagonists may have a capacity to exert a bipartite attack on both the tumor and its neovasculature. However, the potential contribution of an antiangiogenic effect *in vivo* will require additional studies.

If the presence or even the level of expression of the σ-1 receptor are not sufficient to determine susceptibility to σ antagonists, we hypothesized that the way in which the receptor is coupled may determine the biological response. Susceptible cells display a rapid elevation in $[Ca^{2+}]_i$, which is followed hours or even days later by engagement of the apoptotic program, in response to σ antagonists. It is perhaps counterintuitive that the σ-1 antagonists rimcazole and IPAG elevate $[Ca^{2+}]_i$; this would, however, be consistent with antagonist-mediated derepression of a calcium flux mechanism that is held in restraint by the σ-1 receptor. This is supported by our demonstration that the σ-1 agonists (+)-SKF10,047 and (+)-pentazocine oppose the σ-1 antagonist-mediated calcium rise in tumor cells. Reminiscent of this is the tonic inhibition of Ca^{2+} currents in neurons by the CB1 cannabinoid receptor (45) and tonic inhibition of a voltage-gated K^+ channel by the σ-1 receptor (46). It will be interesting now to explore whether there is any cross-talk between calcium and potassium channels in the context of apoptosis induction by σ-1 antagonists. It is clear, however, that the σ-1 receptor does not always hold calcium in restraint because σ-1 agonists elevate intracellular calcium in the presynaptic terminals of normal hippocampal neurons, an effect that is blocked by σ-1 antagonists (47). Taken together, these data suggest that the σ-1 receptor may be somehow inversely coupled in tumor cells and other cells that display a degree of self-reliance, compared with normal neurons. This might help to explain the low toxicity of σ-1 antagonists for normal cells.

In addition to an elevation in $[Ca^{2+}]_i$ and subsequent activation of PLC, σ-1 antagonists inhibit the activity of PKB/Akt in an apparently calcium-independent manner. Thus, PLC activation and PKB/Akt inhibition in response to σ-1 antagonists appear to constitute biochemically separable signal transduction responses that lie upstream of execution of the apoptotic program. This separability suggests that the σ-1 receptor acts both to restrain a proapoptotic signaling pathway and to stimulate a prosurvival signaling cascade that is at least partly independent of the former. The rapidity of the decline in $PtdIns(3,4,5)P_3$ levels (within 5 min after exposure to σ antagonists) additionally shows that the effect on the phosphatidylinositol 3′-kinase pathway is a specific signaling response and not a nonspecific result of a decline in cell viability

The evidence therefore indicates that the σ-1 receptor is differentially coupled in susceptible compared with nonsusceptible cells, but how this is achieved remains to be determined. It is now known that five different isoforms of the σ-1 receptor exist, generated though alternative splicing.[7] It is tempting to speculate that specific isoforms may be differentially coupled to downstream signaling pathways, a possibility we propose to address.

To our knowledge, there are no reported associations between antipsychotic use and anticancer effects in the clinic. This is, however, consistent with our finding that haloperidol—an antipsychotic used in the clinic—has only weak antitumor effects *in vivo* (Fig. 6*A*). This is possibly because haloperidol, along with other currently used antipsychotics, displays σ receptor antagonism as only one of its neuroactive properties, and these may be counteracting the σ antagonist-mediated antitumor effects. Antipsychotics in general may also display σ binding properties that are not sufficiently optimized for living tumor cells.

In conclusion, we speculate that a proapoptotic pathway signaled by calcium may exist as an obligate safeguard to prevent cell-autonomous survival in cell types that possess functional autocrine survival signaling pathways such as microvascular endothelial and lens epithelial cells; tumor cells could, however, be similarly burdened. An Achilles heel could thereby be presented through which to unleash apoptosis in tumor and selected normal cells such as microvascular cells, nonrecovery perhaps being assisted by concomitant inhibition of PKB/Akt prosurvival signaling. Such an approach could conceivably offer a way to kill tumors while sparing normal tissues. Our *in vivo* data give cause for hope that this may be so.

ACKNOWLEDGMENTS

We thank the Developmental Therapeutics Program (NCI) for conducting the rimcazole cytotoxicity screen in the NCI60 panel and for provision of σ-1 receptor microarray data. We also thank Roland Wolf for support of the *in vivo* antitumor studies and Alex Gray for provision of the GFP-PH PLCδ domain protein.

REFERENCES

1. Vilner BJ, John CS, Bowen WD. Sigma-1 and sigma-2 receptors are expressed in a wide variety of human and rodent tumor cell lines. Cancer Res 1995;55:408–13.
2. Everaert H, Flamen P, Franken PR, Verhaeghe W, Bossuyt A. Sigma-receptor imaging by means of I^{123}-IDAB scintigraphy: clinical application in melanoma and non-small cell lung cancer. Anticancer Res 1997;17:1577–82.
3. John CS, Bowen WD, Fisher SJ, et al. Synthesis, *in vitro* pharmacological characterization, and preclinical evaluation of *N*-[2-(1′piperidinyl)ethyl]-3-[^{125}I]iodo-4-methoxybenzamide(P[^{125}I]MBA) for imaging breast cancer. Nucl Med Biol 1999; 26:377–82.
4. Walker JM, Bowen WD, Walker FO, Matsumoto RR, de Costa B, Rice KC. Sigma receptors: biology and function. Pharm Rev 1990;42:355–402.
5. Kekuda R, Prasad PD, Fei YJ, Leibach FH, Ganapathy V. Cloning and functional expression of the human type sigma receptor (hSigmaR1). Biochem Biophys Res Commun 1996;229:553–8.
6. Mei J, Pasternak GW. Sigma1 receptor modulation of opioid analgesia in the mouse. J Pharmacol Exp Ther 2002;300:1070–4.
7. King M, Pan YX, Mei J, Chang A, Xu J, Pasternak GW. Enhanced kappa-opioid receptor-mediated analgesia by antisense targeting the sigma1 receptor. Eur J Pharmacol 1997;331:R5–6.
8. Vilner BJ, De Costa BR, Bowen WD. Cytotoxic effects of sigma ligands: sigma receptor-mediated alterations in cellular morphology and viability. J Neurosci 1995; 15:117–34.
9. Brent PJ, Pang GT. Sigma binding site ligands inhibit cell proliferation in mammary and colon carcinoma cell lines and melanoma cells in culture. Eur J Pharmacol 1995;278:151–60.
10. Brent PJ, Pang G, Little G, Dosen PJ, Van Helden DF. The sigma receptor ligand, reduced haloperidol, induces apoptosis and increases intracellular free calcium levels $[Ca^{2+}]_i$ in colon and mammary adenocarcinoma cells. Biochem Biophys Res Commun 1996;219:219–26.
11. Crawford KW, Bowen WD. Sigma-2 receptor agonists activate a novel apoptotic pathway and potentiate antineoplastic drugs in breast tumor cell lines. Cancer Res 2002;62:313–22.
12. Crawford KW, Coop A, Bowen WD. Sigma(2) receptors regulate changes in sphingolipid levels in breast tumor cells. Eur J Pharmacol 2002;443:207–9.

[7] Internet address: http://www.ncbi.nlm.nih.gov/LocusLink.

13. Berthois Y, Bourrié B, Galiègue S, et al. SR31747A is a sigma receptor ligand exhibiting antitumoural activity both *in vitro* and *in vivo*. Br J Cancer 2003;88:438–46.
14. Kerr JFR, Wyllie AH, Currie AR. Apoptosis: a basic biological phenomenon with wide-ranging implications in tissue kinetics. Br J Cancer 1972;26:239–57.
15. Raff MC. Social controls on cell survival and cell death. Nature (Lond.) 1992;356: 397–400.
16. Weil M, Jacobson MD, Coles HS, et al. Constitutive expression of the machinery for programmed cell death. J Cell Biol 1996;133:1053–9.
17. Evan GI, Vousden KH. Proliferation, cell cycle and apoptosis in cancer. Nature (Lond.) 2001;411:342–8.
18. Green DR, Evan GI. A matter of life and death. Cancer Cell 2002;1:19–30.
19. Courtney MJ, Lambert JJ, Nicholls DG. The interactions between plasma membrane depolarization and glutamate receptor activation in the regulation of cytoplasmic-free calcium in cultured cerebellar granule cells. J Neurosci 1990;10:3873–9.
20. Wiegand UK, Corbach S, Prescott AR, Savill J, Spruce BA. The trigger to cell death determines the efficiency with which dying cells are cleared by neighbours. Cell Death Differ 2001;8:734–46.
21. Leslie NR, Bennett D, Gray A, Pass I, Hoang-Yuan K, Downes CP. Targeting mutants of PTEN reveal distinct subsets of tumour suppressor functions. Biochem J 2001;357:427–35.
22. Batty IH, Downes CP. Thrombin receptors modulate insulin-stimulated phosphatidylinositol 3,4,5-trisphosphate accumulation in 132N1 astrocytoma cells. Biochem J 1996;317:347–51.
23. Estevez F, Pulford D, Stark MJR, Carter NA, Downes CP. Inositol trisphosphate metabolism in Saccharomyces cerevisiae: identification, purification and properties of inositol 1,4,5,-trisphosphate 6-kinase. Biochem J 1994;302:709–16.
24. Ferris RM, Tang FL, Chang KJ, Russell A. Evidence that the potential antipsychotic agent rimcazole (BW234U) is a specific, competitive antagonist of sigma sites in brain. Life Sci 1986;38:2329–37.
25. Wilson AA, Dannais RF, Ravert HT, Sonders MS, Weber E, Wagner HN Jr. Radiosynthesis of σ receptor ligands for positron emission tomography: ^{11}C- and ^{18}F-labelled guanidines. J Med Chem 1991;34:1867–70.
26. Klein M, Cooper TB, Musacchio JM. Effects of haloperidol and reduced haloperidol on binding to sigma sites. Eur J Pharmacol 1994;254:239–48.
27. Matsumoto RR, Bowen WD, Tom MA, Vo VN, Truong DD, de Costa BR. Characterisation of two novel sigma receptor ligands: antidystonic effects in rats suggest sigma receptor antagonism. Eur J Pharmacol 1995;280:301–10.
28. Matsuno K, Senda T, Mita S. Correlation between potentiation of neurogenic twitch contraction and benzomorphan sigma receptor binding potency in the mouse vas deferens. Eur J Pharmacol 1993;231:451–7.
29. Matsuno K, Kobayashi T, Mita S. Involvement of sigma receptors in the increase in contraction of mouse vas deferens induced by exogenous ATP. J Pharm Pharmacol 1996;48:96–9.
30. Vilner BJ, Bowen WD. Modulation of cellular calcium by sigma-2 receptors: release from intracellular stores in human SK-N-SH neuroblastoma cells. J Pharm Exp Ther 2000;292:900–11.
31. De Coster MA, Klette KL, Knight ES, Tortella FC. Sigma receptor-mediated neuroprotection against glutamate toxicity in primary rat neuronal cultures. Brain Res 1995;671:45–53.
32. Langa F, Codony X, Tovar V, et al. Generation and phenotypic analysis of sigma receptor type 1 (σ1) knockout mice Eur J Neurosci 2003;18:2188–96.
33. Hayashi T, Su T-P. Regulating ankyrin dynamics: roles of sigma-1 receptors. Proc Natl Acad Sci USA 2001;98:491–6.
34. Jänicke RU, Sprengart ML, Wati MR, Porter AG. Caspase-3 is required for DNA fragmentation and morphological changes associated with apoptosis. J Biol Chem 1998;273:9357–60.
35. Talanian RV, Quinlan C, Trautz S, et al. Substrate specificities of caspase family proteases. J Biol Chem 1997;272:9677–82.
36. Starr JB, Werling LL. σ receptor up-regulation of [^{3}H]arachidonic acid release from rat neonatal cerebellar granule cells in culture. J Neurochem 1994;63:1311–8.
37. Berridge MJ, Bootman MD, Lipp P. Calcium: a life and death signal. Nature (Lond.) 1998;395:645–8.
38. Tombal B, Denmeade SR, Gillis J-M, Isaacs JT. A supramicromolar elevation of intracellular free calcium ([Ca^{2+}]$_i$ is consistently required to induce the execution phase of apoptosis. Cell Death Differ 2002;9:561–73.
39. Nash MS, Young W, Willars GB, Challiss RA, Nahorski SR. Single-cell imaging of graded Ins(1,4,5,)P_3 production following G-protein-coupled receptor activation. Biochem J 2001;356:137–42.
40. Kim YH, Park TJ, Lee YH, et al. Phospholipase C-delta 1 is activated by capacitative calcium entry that follows phospholipase C-beta activation upon bradykinin stimulation. J Biol Chem 1999;274:26127–34.
41. Li J, Yen C, Liaw D, et al. PTEN, a putative protein tyrosine phosphatase gene mutated in human brain, breast, and prostate cancer. Science (Wash. DC) 1997;275:1943–7.
42. Ishizaki Y, Voyvodic JT, Burne JF, Raff MC. Control of lens epithelial cell survival. J Cell Biol 1993;121:899–908.
43. Scholzen TE, Brzoska T, Kalden DH, et al. Expression of functional melanocortin receptors and proopioimelanocortin peptides by human dermal microvascular endothelial cells. Ann NY Acad Sci 1999;885:239–53.
44. Li A, Dubey S, Varney ML, Dave B, Singh RK. IL-8 directly enhanced endothelial cell survival, proliferation, and matrix metalloproteinases production and regulated angiogenesis. J Immunol 2003;170:3369–76.
45. Pan X, Ikeda SR, Lewis DL. SR141716A acts as an inverse agonist to increase neuronal voltage-dependent Ca^{2+} currents by reversal of tonic CB1 cannabinoid receptor activity. Mol Pharmacol 1998;54:1064–72.
46. Aydar E, Palmer CP, Klyachko VA, Jackson MB. The sigma receptor as a ligand-regulated auxiliary potassium channel subunit. Neuron 2002;34:399–410.
47. Meyer DA, Carta M, Partridge LD, Covey DF, Valenzuela CF. Neurosteroids enhance spontaneous glutamate release in hippocampal neurons. J Biol Chem 2002; 277:28725–32.